# **Research Article**

# The impact of ionising radiation from geophysical loggers and water content on the luminescence signals in sediment cores

Sam Woor<sup>a,b</sup>, Alex Hughes<sup>b</sup>, Mitch K. D'Arcy<sup>b</sup>, Olav B. Lian<sup>a</sup>, Cooper D. Stacey<sup>c</sup> and Randolph J. Enkin<sup>c</sup>

<sup>a</sup>Department of Geoscience, University of the Fraser Valley, Abbotsford, BC, Canada; <sup>b</sup>Department of Earth, Ocean and Atmospheric Sciences, University of British Columbia, Vancouver, Canada and <sup>c</sup>Geological Survey of Canada, Sidney, Canada

#### **Abstract**

Luminescence dating and profiling are important analytical methods for providing chronological constraints and reconstructing depositional histories from sediment cores. However, sediment cores have often been exposed to ionising radiation sources during geophysical analyses, which potentially contaminates natural luminescence signals and may compromise the accuracy and reliability of luminescence analyses. Variable water content down-core is another potential issue for the rapid analysis of sediments, as water attenuates luminescence and may limit the comparability of samples. Here, we use a portable optically stimulated luminescence reader to test the influence of two common geophysical analyses—X-radiography and gamma-ray logging—on the luminescence properties of sediments in marine cores. We demonstrate that both techniques cause negligible changes to luminescence signals with doses <100 mGy. We test the effect of variable water content on luminescence and show that net signals are reduced by up to 70% at 30% moisture, relative to dry sediments. Accurate and reliable luminescence signals can be obtained from sediment cores despite prior exposure to ionising radiation from geophysical loggers or variable water content. However, the accuracy of luminescence measurements does require taking appropriate steps before analysis, like assessing the doses given by geophysical instruments at specific laboratories or drying samples.

Keywords: optically stimulated luminescence dating; sedimentology; geomorphology; geochronology; pOSL; quaternary

# Introduction

Luminescence is a phenomenon whereby certain minerals emit photons of light upon exposure to heat or daylight. This is due to the recombination of electrons held at meta-stable states through exposure to ionising radiation in the environment during their burial. Optically stimulated luminescence dating uses this phenomenon to estimate the time elapsed since quartz and potassiumrich feldspar grains were last exposed to daylight (Huntley et al., 1985; Murray et al., 2021). Luminescence dating has provided chronological control for cores obtained from a range of terrestrial sedimentary settings, like aeolian dunes (e.g., Stokes and Bray, 2005), floodplains (e.g., Pears et al., 2020), and lakes (e.g., Burrough et al., 2009). In marine environments, luminescence applications are more limited due to the lower likelihood of luminescence signals being fully reset by daylight in deep-water environments, as well as the authigenic uptake of uranium in deep-sea sediments rendering traditional environmental dose rate calculations inappropriate (Armitage, 2015). Nevertheless, studies have successfully applied luminescence dating to horizons in marine sediment cores that have been sufficiently reset before deposition (e.g., Wintle

Corresponding author: Sam Woor; Email: samuel.woor@ufv.ca

Cite this article: Woor, S., Hughes, A., D'Arcy, M.K., Lian, O.B., Stacey, C.D., Enkin, R.J., 2025. The impact of ionising radiation from geophysical loggers and water content on the luminescence signals in sediment cores. *Quaternary Research*, 1–13. https://doi.org/10.1017/qua.2025.10035

and Huntley, 1979; Stokes et al., 2003; Berger, 2009; Armitage and Pinder, 2017; Kluesner et al., 2023).

In addition to age information, luminescence signals measured from sediment cores contain information about past environments and sedimentary processes. As such, "luminescence profiling" is increasingly applied to sediment cores as a novel proxy for variables such as mineralogy, provenance, and palaeoenvironmental changes (Munyikwa et al., 2021). Recent developments in luminescence profiling have, in part, been facilitated by the availability of the portable optically stimulated luminescence (pOSL) readers developed by the Scottish Universities' Environmental Research Centre (Sanderson and Murphy, 2010). Designed to measure both the infrared-stimulated luminescence (IRSL) and blue optically stimulated luminescence (BOSL) signals from bulk sediment, pOSL readers can rapidly generate luminescence profiles through cores to provide stratigraphic insights or as an initial screening before full luminescence dating is applied. For example, pOSL profiling of archived core material from Lake Suigetsu, Japan, has been used to identify historic flood layers by the detection of luminescence signal "spikes" related to poor signal resetting during turbulent sediment transport (Rex et al., 2022). In the same location, pOSL profiling has identified stratigraphic breaks, in one case attributed to a palaeoearthquake that changed the sources of sediment supplied to the lake (Staff et al., 2024). Increases in pOSL signals have also been used to identify periods of poorly bleached sediment deposition in cores taken from the floodplain of the River Severn, UK (Pears et al., 2020). These pOSL signals

© The Author(s), 2025. Published by Cambridge University Press on behalf of Quaternary Research Center. This is an Open Access article, distributed under the terms of the Creative Commons Attribution licence (http://creativecommons.org/licenses/by/4.0), which permits unrestricted re-use, distribution and reproduction, provided the original article is properly cited.

are indicative of increased soil erosion corresponding with greater agricultural activity during the Late Iron Age and Romano-British period (2000–1800 yr BP), as well as warmer and wetter conditions during the Medieval Climate Anomaly (1100–600 yr BP; Pears et al., 2020).

These examples illustrate the opportunities for using pOSL readers to characterise sediment cores and learn about depositional histories, processes, and environments. Given the logistical and financial effort involved in retrieving sediment cores, especially from subaqueous environments, they are often stored for many years in repositories. Archived cores can be suitable for luminescence dating and profiling studies, even many years after they were first split (e.g., Armitage and Pinder, 2017). However, there are three potential problems in applying luminescence methods to sediment cores.

First, luminescence signals are rapidly reset by daylight exposure, often within seconds (Murray et al., 2012). Light exposure could therefore deplete the natural luminescence signals within cores once they have been opened and exposed to wavelengths of light outside the yellow/orange and red wavelengths that are typically considered to cause negligible signal resetting in luminescence laboratories (Sohbati et al., 2017). Encouragingly, Armitage and Pinder (2017) demonstrated that daylight exposure did not significantly alter the luminescence signals obtained from sediment 1 mm below the split face of a marine core. Although only one example, this result suggests that archived cores may still yield accurate luminescence data despite prior light exposure during core splitting and sampling, so long as a few millimetres of light-exposed surficial material are first removed. Another cause of potential luminescence signal bleaching in stored sediment cores is the opening up of small cracks due to drying. Bleaching due to cracking is harder to deal with than simply removing the top layer of sediment from a split surface. So, it is important to make a detailed inspection of the core barrel (if translucent) and the split surface to identify any horizons potentially effected by cracking before sampling.

The second challenge is the potential effect of ionising radiation sources within geophysical core loggers on luminescence signals. Multisensor core loggers (MSCL) provide automated geophysical logging with a variety of in-built, multiproxy sensors (e.g., gamma ray, magnetic susceptibility, p-wave). Some of these multiproxy techniques utilise radioactive sources and have become standard research methods applied to most cores. For instance, gamma-ray logging is widely used to measure sediment density due to the variable attenuation of gamma rays as they pass through the core (Rothwell and Rack, 2006). Data from MSCLs are often supplemented by X-radiography, which provides high-resolution imaging of the internal structure of core sediments (Algeo et al., 1994), and X-ray fluorescence (XRF), which measures elemental concentrations along the split face of a core (Weltje and Tjallingii, 2008). Many of these methods are non-invasive, meaning that they can be applied without the need to split cores, and are typically considered nondestructive because they preserve core material for subsequent analyses. While physically "nondestructive," exposing sediments to ionising radiation adds an additional radiation dose beyond what would be found in nature.

In principle, these techniques could potentially increase luminescence signals and thereby render luminescence dating or profiling inaccurate when performed before luminescence analysis. Unfortunately, few constraints are available about the impact that core loggers have on natural luminescence signals, especially for un-split sediment cores. Davids et al. (2010) measured doses of

up to 0.61 Gy and 2.51 Gy at the surface of a split sediment core delivered by X-radiograph and XRF systems, respectively. These delivered doses decreased with depth into the core to <0.01 Gy at 30 mm and also varied depending on lateral position across the core, relative to the X-ray source, with the highest doses delivered in the centre. Moreover, there has been no prior research into the impact of artificially dosing sediment cores on the signals and metrics commonly used in luminescence profiling studies. For example, measurements of signal depletion rate and the ratio of IRSL to BOSL are increasingly obtained using pOSL readers and used as proxies for changing sediment provenance and mineralogy (e.g., Robins et al., 2021; Adolph et al., 2022). However, the sensitivity of these metrics to the dosing associated with standard core analyses remains unknown.

The third issue is the influence of variable water content throughout sediment cores on luminescence profiling studies. Water attenuates the luminescence signals read by pOSL readers from bulk sediments (Bateman et al., 2015). For example, a reduction in net BOSL counts by up to 24% with increasing water content up to 0.73%, relative to the signal from dry sediment, was reported for aeolian sand in the Thar Desert, northern India (Nitundil et al., 2023). Cores from marine or floodplain settings will likely contain greater amounts of moisture, with marine sediments often exceeding 40% water content (e.g., Tjallingii et al., 2007). Down-core, water content can vary considerably due to differences in sediment porosity and compaction, with sediment in the uppermost portions of cores from subaqueous environments typically having the greatest water content (e.g., Hennekam and de Lange, 2012). The storage conditions of cores can also influence water content, for instance vertical storage can result in the upper portions of cores drying out and the lower portions becoming saturated. Therefore, water content variability may limit the comparability of samples when conducting luminescence profiling studies on cores, especially for marine and lacustrine records several metres long.

In this study, we test the impact of X-rays, gamma rays, and water content on pOSL data obtained from marine sediment cores. We use sediment collected from the centre of cores to measure a range of commonly used luminescence metrics and compare the results before and after exposure to ionising radiation. We also use retrospective dosimetry to estimate the dose received by these sediments during irradiation. Finally, we test the influence of water content on pOSL measurements across a range of values that are representative of marine, lacustrine, and floodplain sediment cores.

## **Methods**

## Core samples

Short (~20–30 cm), 10-cm-diameter sediment cores were collected from the Bute Inlet, southwestern British Columbia, using a box corer onboard the research vessel CCGS *Vector* in 2016 (Fig. 1a). The Bute Inlet is a fjord fed primarily from the north and east by the Homathko and Southgate Rivers, respectively. The inlet is 78 km long with an average depth of 550 m (Hage et al., 2022). Since collection, duplicate cores have been stored, unopened, at the Pacific Geoscience Centre's core storage facility in Saanich, British Columbia. Before sampling, the unopened, transparent core barrels were inspected for any visible cracks in the stored sediment. Any depths where cracking was evident were avoided when the cores were sampled.

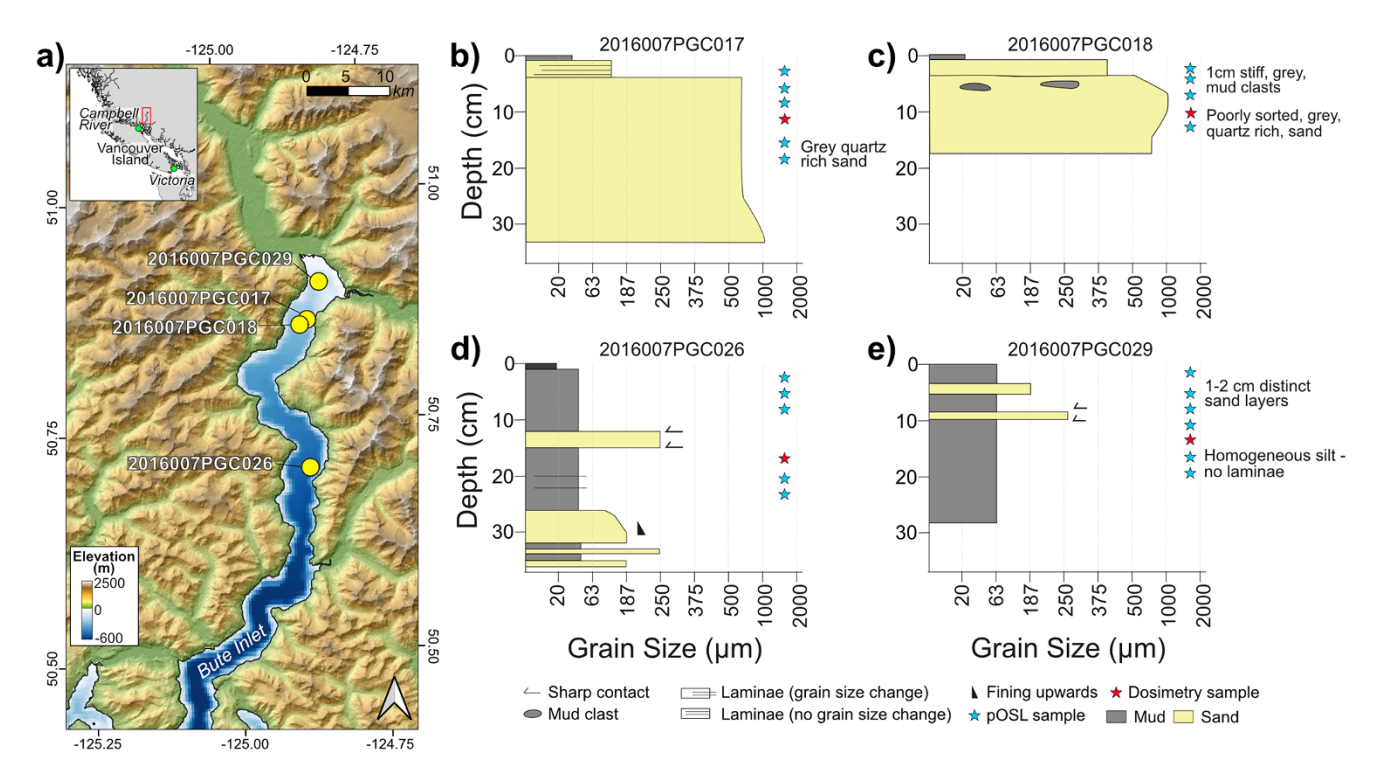


Figure 1. (a) Map of the Bute Inlet in British Columbia, Canada, showing the location of box cores (yellow points) used for this study. (b-e) Stratigraphic logs of the four box cores showing grain size, sedimentary structures, and the horizons sampled for portable optically stimulated luminescence (pOSL) analyses and the placement of dosimeters.

For this study, four cores were selected based on their predominate grain size: two majority sand-sized samples (cores 2016007PGC017 and 2016007PGC018; Fig. 1b and c) and two finer-grained samples, majority silty mud (cores 2016007PGC026 and 2016007PGC029; Fig. 1d and e). Targeting different particle sizes provided an opportunity to compare the shielding effects for different grain sizes and sediment densities upon exposure to the external ionising radiation sources.

# Testing the impact of geophysical core logging

## Geophysical logging equipment

The impact of two sources of ionising radiation that are commonly used for the geophysical logging of sediment cores were tested in this study. First, we tested a Geotek Multisensor Core Logger equipped with an Eckert and Zeigler CS7.P03 system for measuring sediment density. This system holds a gamma-ray-emitting <sup>137</sup>Cs source with a current activity of 256 MBq, and the detector is comprised of a cylindrical 7.5-cm-diameter, 15-cm-long scintillation crystal of NaI(TI). Emitted gamma rays are collimated to a 0.5-cm-diameter beam. Cores were passed horizontally through the logger at a distance of 15 cm from the <sup>137</sup>Cs source with an integration time of a 6 s pause at each centimetre increment along the core.

Second, we tested the impact of a Universal HE425 X-radiography system equipped with a Toshiba UX-52H-39 X-ray tube. This system operates with 100 mA at 100 kV for a duration of 0.5 s. Sediment cores were positioned horizontally underneath the X-ray source at a distance of 96 cm.

## pOSL profiling signals

Cores were split under subdued, red-light conditions to ensure that luminescence signals were not reset during sampling. We pressed 1-cm-diameter and 0.2-cm-deep, straight-sided aluminium planchets into the split face of the core (Fig. 2a). The aliquots were packed and levelled off so that the grains were flush with the sides of the planchet, helping to maximise sample comparability by standardising the distance between the sample and photomultiplier tube. For the silt-sized sediments, with an assumed mean grain size of 33.2  $\mu m$ , we estimate that an average of 58,397  $\pm$ 14,762 grains could be included across the surface of each aliquot. For very fine to fine sand-sized sediments, with an assumed mean grain size of 156.3  $\mu$ m, we estimate that an average of 2623  $\pm$  661 grains could be included across the surface of each aliquot. These values were calculated using the calc\_AliquotSize function in the Luminescence R package (Kreutzer et al., 2012), assuming the default packing density of 0.65. The aliquots measured in this study, therefore, include more grains than are typically measured in traditional luminescence dating studies (Duller, 2008a), but fewer grains than are often measured in other pOSL studies where aliquots of 5 cm diameter are commonly used (e.g., Gray et al., 2019; Stone et al., 2019; Rex et al., 2022).

Sampling positions were spaced at various horizons down one half of the split core, with three samples taken across each horizon (positions A–C) to test the lateral variability of luminescence signals (Davids et al., 2010). We avoided the outermost 1 cm of sediment to minimise the potential effects of barrel smearing at the edge of the core (Armitage and Pinder, 2017). To ensure comparable sample sizes, we levelled off extracted samples to be flush with the walls of the planchet. Samples were stored in light-proof containers before analysis.

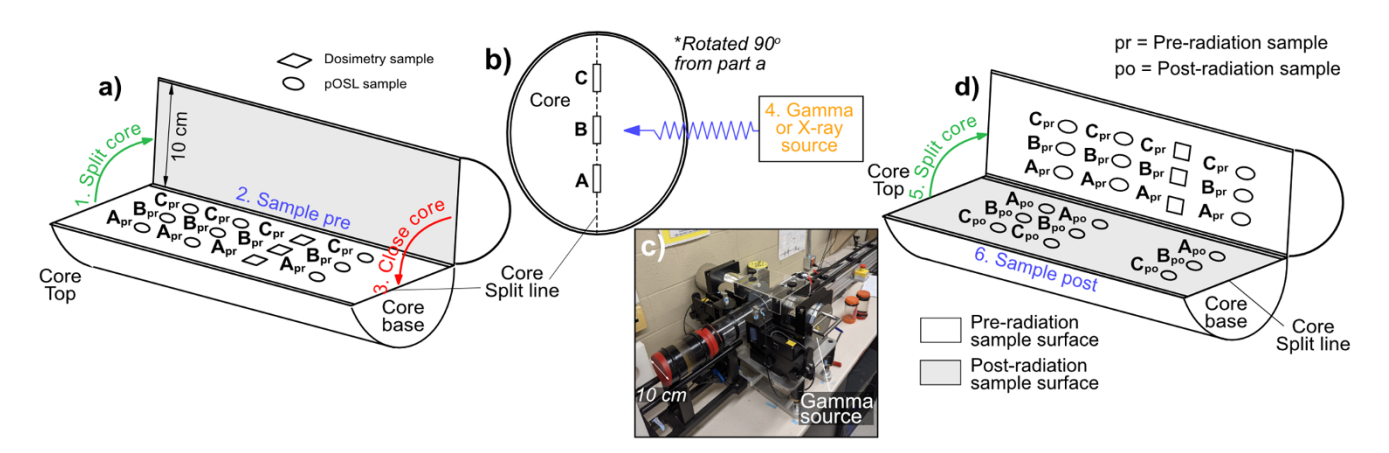


Figure 2. The sampling approach taken in this study. (a) Three samples were taken from locations (A, B, and C) along one face of the split core under subdued red light. Dosimetry packages were also arranged across one sampling row. (b and c) The core, rotated 90° on its long axis, was exposed to gamma or X-rays in either a multisensor core logger or X-radiograph, respectively. (d) The core was reopened under subdued red light, the dosimetry packages were removed, and samples were taken from the opposing face at the same depth and lateral positions as in a. pOSL, portable optically stimulated luminescence.

After initial sampling, cores were carefully closed and made light-proof with opaque electrical tape (Fig. 2b). We then passed one sandy core (core 2016007PGC018) and one fine-grained core (core 2016007PGC029) through the MSCL equipped with a gamma-ray source with a 6 s pause at 1 cm intervals (Fig. 2c). We imaged cores 2016007PGC017 (sand) and 2016007PGC026 (fine-grained) with the X-radiograph. To ensure comparability, we arranged all cores so that the split face inside the core was perpendicular to the gamma- or X-ray source. Following exposure of cores to the radiation sources, we reopened them under subdued, red-light conditions (Fig. 2d) and resampled following the same procedure as before but targeting the opposing face of the split core, mirroring the samples taken pre-exposure.

The luminescence signals of all samples were measured using a Scottish Universities Environmental Research Centre (SUERC) pOSL reader. For consistency with other pOSL studies, we applied the "constant-wave proxies" (CW-proxies) measurement protocol (Sanderson and Murphy, 2010; Table 1). Along with net IRSL and BOSL counts (the sum of the two 30 s IRSL and BOSL stimulations minus the pre- and proceeding dark counts; Table 1), the CWproxies protocol provides additional luminescence metrics that correspond to changes in sediment provenance and mineralogy (e.g., Munyikwa et al., 2021; Stone et al., 2024). The IRSL/BOSL ratio is simply the ratio of the net IRSL and net BOSL counts. The depletion ratios measure the rate at which the IRSL and BOSL signals deplete by dividing the net counts of the first 30 s measurement by the second 30 s measurement (Table 1). Stimulation was applied using light-emitting diodes (LEDs), which included 880 nm IR light (90 mW) and 470 nm blue light (25 mW). During measurement, planchets were positioned in the centre of a 5 cm petri dish swabbed with clear Silkospray silicon oil (which does not influence the luminescence signals) to ensure that they did not move during the opening and closing of the sample drawer and to establish a standard distance between samples and the photomultiplier tube to reduce inter-sample variability due to differences in instrumental setup.

To test whether instrumental setup is a significant source of variability for repeat aliquots, we measured 10 aliquots of Morar Sand spread over a 9.8 mm aluminium disc with the CW-proxies procedure. Morar Sand is a well-bleached, quartz-rich, Holocene sand from an estuary in western Scotland that is supplied as a

reference material by SUERC for pOSL readers (Schmidt et al., 2021). These aliquots yielded a mean BOSL signal of 2601.1  $\pm$  133.4 counts, with an overdispersion of 17  $\pm$  4 %, and the IRSL signals yielded a mean of 6019.4  $\pm$  250.1 counts with an overdispersion of 14  $\pm$  3 %. The low standard errors, relative to the mean counts, as well as the low overdispersions (<20 %), suggest that, for a sample that is known to be well-bleached and compositionally homogenous, the instrumental inter-sample variability is low for our experimental setup. We also conducted empty chamber measurements before and in between samples to monitor potential contamination.

## Quartz dosimetry

We devised a simple experiment to estimate the doses delivered to the core sediments during geophysical logging. For a retrospective dosimeter, we used calibration quartz supplied by Risø (batch 90), which has been sieved to  $180\text{--}250~\mu m$ , etched with hydrofluoric acid, and given a 0 Gy dose. Risø calibration quartz is commonly used for beta-source calibration in luminescence dating laboratories (Hansen et al., 2018). The quartz is extracted from bulk sediments sourced from aeolian dunes on the west coast of Denmark and has been sensitised through various cycles of thermal annealing and exposure to a gamma-ray source (Hansen et al., 2015). A final thermal annealing cycle ensures that any residual OSL signals are reset, and it has been demonstrated that this quartz can accurately measure doses from  $10^{-3}\text{--}10^2$  Gy irrespective of preheat temperatures between  $160^{\circ}\text{C}$  and  $260^{\circ}\text{C}$  (Hansen et al., 2015).

To make the dosimeters, we dispensed small amounts of calibration quartz onto 4 x 2 cm tabs of Scotch tape, which were then folded in half to form sealed packages. After splitting the cores for pOSL sampling (see "pOSL Profiling Signals"), we placed three of these dosimetry packages across one horizon in each core and secured them in place with electrical tape before resealing the cores (Fig. 2a). We ensured the dosimeters aligned with pOSL sample positions (A–C) and passed them through the geophysical loggers to simulate the exposure of natural sediments in the centre of cores to ionising radiation.

The quartz packages were removed from the core and soaked in de-ionised water for 24 hours to soften the adhesive on the tape, then gently opened, and the grains were scraped out and left

**Table 1.** The "constant-wave proxies" (CW-proxies) and quartz dosimetry protocols used for luminescence measurements. Carbon counts' are periods during which the photomultiplier tube is actively counting photons without LED stimulation to measure background signals. The dark counts before and after IRSL and BOSL measurements were subtracted from IRSL and BOSL counts before they were used to calculate the metrics.

	Measurement protocol						
		CW-proxies	Quartz dosimetry				
Measurement step	Measured	Description	Measured	Description			
1	Dark count (30 s)	Background photon counts used to correct signals	Preheat (180 °C, 10 s) <sup>ab</sup>	Heating to empty unstable traps			
2	IRSL (30 s)	Used to calculate net IRSL counts ([Step 2 – dark counts] + [Step 3 – dark counts]), IRSL	Dark count (30 s)	Same as Step 1			
3	IRSL (30 s)	depletion ([Step 2 – dark counts] $\div$ [Step 3 – dark counts]), and the IRSL/BOSL ratio (net IRSL counts $\div$ net BOSL counts)	BOSL (60 s)	Measurement of the post-exposure signal			
4	Dark count (30 s)	Same as Step 1	Dark count (30 s)	Same as Step 1			
5	BOSL (30s)	Used to calculate net BOSL counts ([Step 5 – dark counts] + [Step 6 – dark counts]), BOSL depletion ([Step 5 – dark counts] ÷ [Step 6 –	Give regenerative dose (0.5 Gy) <sup>ab</sup>	Test dose applied to normalise the signal measured in Step 2			
6	BOSL (30 s)	dark counts]), and the IRSL/BOSL ratio (net IRSL counts $\div$ net BOSL counts)	Preheat (180 °C, 10 s) <sup>ab</sup>	Heating to empty unstable traps			
7	Dark count (30 s)	Same as Step 1	Dark count (30 s)	Same as Step 1			
8			BOSL (60 s)	Measurement of the test signal used to normalise the signal measured in Step 2			
9			Dark count (30 s)	Same as Step 1			

<sup>&</sup>lt;sup>a</sup>The "dark counts" are periods during which the photomultiplier tube is actively counting photons without light-emitting diode (LED) stimulation to measure background signals. The dark counts before and after infrared-stimulated luminescence (IRSL) and blue optically stimulated luminescence (BOSL) measurements were subtracted from IRSL and BOSL counts before they were used to calculate the metrics.

to settle in the water. We then removed excess water and rinsed the quartz with acetone to dissolve any residual adhesive before mounting the dried quartz grains as 3-mm-diameter aliquots on 9-mm-diameter aluminium discs for measurement. We measured three aliquots per sample.

To estimate the doses received by the quartz grains, we adapted a protocol used for rapid equivalent dose estimation employed in pOSL studies (Sanderson and Murphy, 2010; Table 1). We first preheated samples to 180°C for 10 s in a Risø TL/OSL DA-20 reader to empty thermally unstable electron traps. Samples were then transferred to the pOSL reader, where they underwent a 60 s stimulation with blue light. The samples were then placed back into the Risø TL/OSL DA-20 reader and given a 0.5 Gy dose from a <sup>90</sup>Sr/<sup>90</sup>Y beta source before another preheat at 180°C for 10 s. We measured the BOSL signal from this test dose with another 60 s stimulation in the pOSL to normalise the initial "natural" signal following exposure to the radiation sources and provide an estimate of the dose received (Steps 3 and 8, respectively; Table 1). We also measured three aliquots of unexposed 0 Gy calibration quartz as a control group. Both BOSL measurements were corrected for a mean empty chamber count, calculated by running the pOSL measurement sequence 10 times without a sample present, due to the sensitivity of the small signals expected to arise from low doses to background noise.

#### Testing the impact of water content

We extracted bulk samples of silty mud and sand from spare Butte Inlet cores that were collected with those shown in Figure 1. The bulk sediment was oven-dried at 30°C and gently disaggregated before being weighed out as 3 g portions into 5-cm-diameter plastic petri dishes. We systematically added de-ionised water by percentage weight of the dry sediment, ranging from 0% to 50% at 5% increments, and mixed it thoroughly to ensure even distribution. We then measured the samples using the CW-proxies protocol (Table 1).

# **Results**

# The effect of geophysical loggers on luminescence signals

pOSL profiling signals

To quantify the change in luminescence parameters due to exposure to ionising radiation, results are expressed as ratios between measured signals after and before radiation exposure. As such, a ratio greater than unity indicates a net increase in the specific luminescence metric following radiation exposure.

Net IRSL and BOSL photon count ratios for the individual sample positions (A, B, and C) at each depth horizon show significant scatter in all four cores (Fig. 3). This scatter likely reflects inherent natural variability resulting from sampling across a small surface area (1 cm²) in water-lain sediment (see discussion in "The Impact of Ionising Radiation Sources on pOSL Metrics"). Despite the magnitude of the scatter, we detect no systematic behaviour for net photon counts between specific positions A, B, and C in any of the four cores (e.g., position B in the centre of the core is not systematically higher than positions A and C; Fig. 3). Therefore, for the

abThese measurement steps were carried out in a Risø TL/OSL DA-20 reader. All other steps were conducted using a portable optically stimulated luminescence (pOSL) pOSL reader.

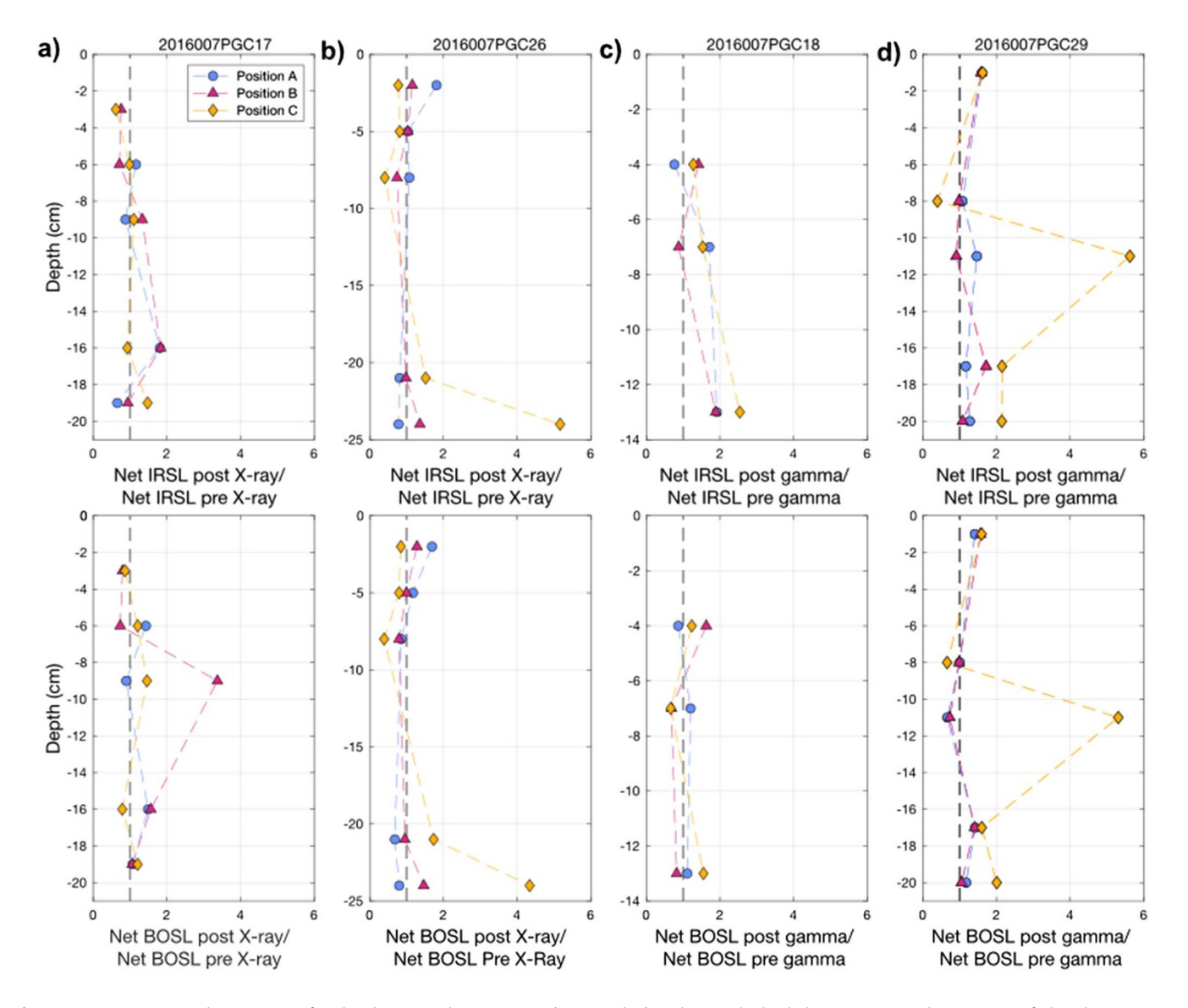


Figure 3. Down-core net photon counts for the three sampling positions (A, B, and C) and at each depth horizon expressed as a ratio of the photon count post-irradiation relative to pre-irradiation. The dashed line represents unity, meaning any ratio above this line has experienced an increase in net photons due to radiation exposure. In each part (a-d) the top plots show the infrared-stimulated luminescence (IRSL) response, and the bottom plots shows the blue optically stimulated luminescence (BOSL) response. (a) Core 2016007PGC17; (b) core 2016007PGC26; (c) core 2016007PGC18; (d) core 2016007PGC29.

following results, we focus on horizon-averaged (mean triplicate) values for the three samples at each depth horizon, but with error bars showing the full variability within the measured data.

Figures 4 and 5 show the luminescence response of sediment following exposure to X-rays in cores 2016007PGC017 (predominantly sand) and 2016007PGC026 (predominantly mud), respectively. Most samples show an increase in horizon-averaged net IRSL and BOSL intensity ratios following X-ray exposure (Figs. 4a and 5a). However, mean signal intensity ratios show scatter around unity, with some showing lower signal intensities following X-ray exposure, and their uncertainties overlap with unity for the majority of sampled horizons. Mean signal intensities generally increase in the sandy core (2016007PGC017) post–X-ray exposure and range from  $0.69 \pm 0.07$  to  $1.52 \pm 0.42$  for IRSL signals and  $0.83 \pm 0.03$  to  $1.91 \pm 1.06$  for BOSL signals (Fig. 4a). By contrast, mean signal intensity ratios for the mud core (2016007PGC026) post–X-ray exposure are scattered around unity, ranging from

 $0.74\pm0.27$  to  $2.44\pm1.95$  for IRSL signals and  $0.67\pm0.21$  to  $2.20\pm1.54$  for BOSL signals (Fig. 5a). For the mud core, mean ratio uncertainties are 11–80% (IRSL) and 16–70% (BOSL), compared with 10–33% (IRSL) and 4–56% (BOSL) for the sandy core (uncertainties calculated as 1 SD as a percentage of the mean).

Exposure to X-rays has almost no effect on the depletion ratios or the IRSL/BOSL ratio (Figs. 4b and c and 5b and c). The IRSL and BOSL depletion ratios for both the sand and mud cores are tightly clustered around unity and within  $\pm 10\%$  in all cases, which means that the measurement changes post–X-ray exposure are statistically insignificant in most cases (Figs. 4b and 5b). The IRSL/BOSL ratios for the sandy core show some variability, with mean post–/pre–X-ray exposure ratios generally less than unity  $(0.71 \pm 0.24 \pm 0.19 \pm 0.02)$  but typically within uncertainties of  $\pm 10\%$  of unity (Fig. 4c). The IRSL/BOSL ratios for the mud core post–X-ray exposure are also very consistent with mean post–/pre–X-ray exposure ratios within  $\pm 10\%$  of unity (Fig. 5c).

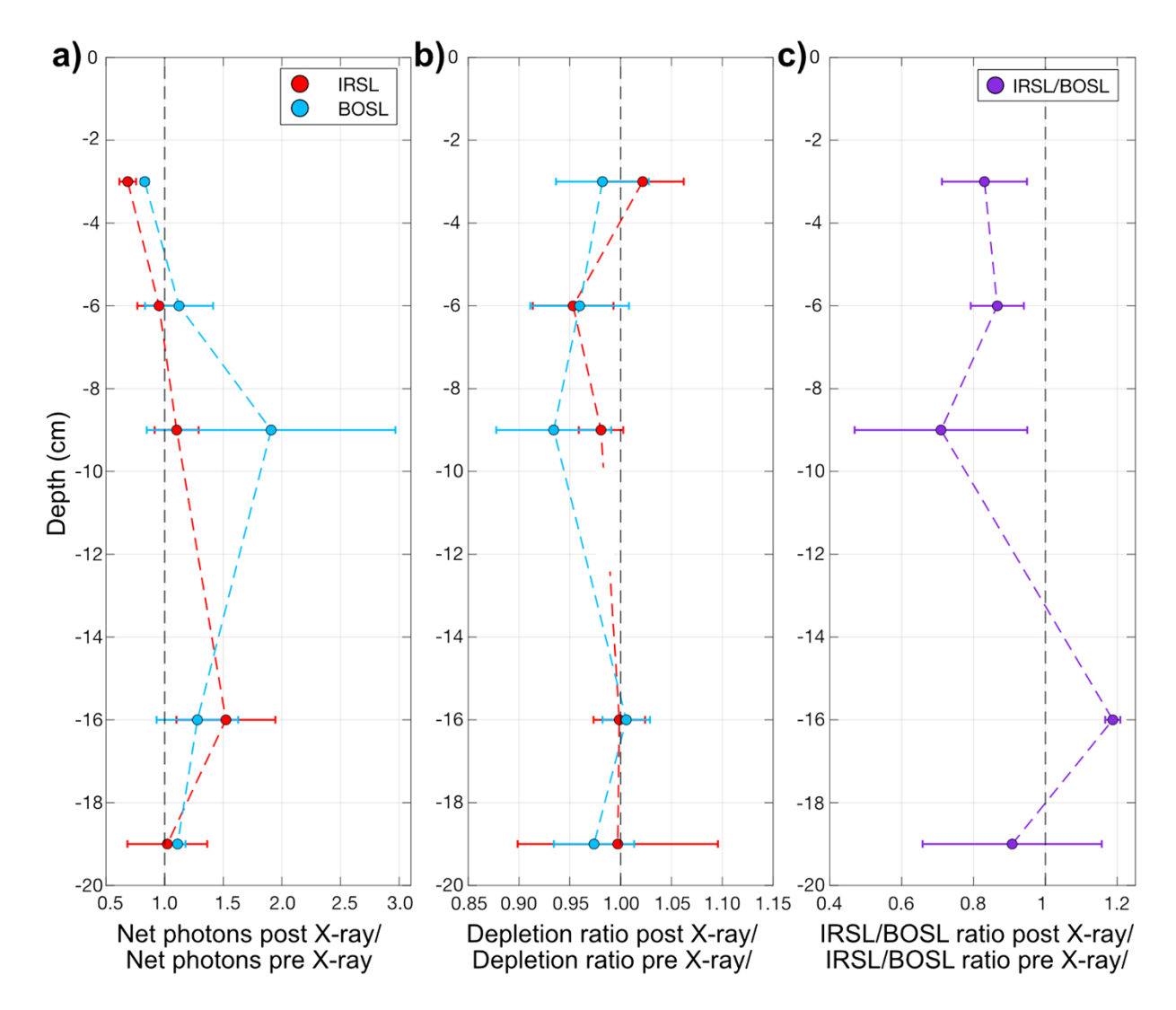


Figure 4. Luminescence data vs. depth, from box core 2016007PGC17 (sand dominated, exposed to X-rays). The values for each luminescence parameter are expressed as a ratio of the parameter post-exposure to X-rays relative to pre-exposure to X-rays. Each point is an average from each depth horizon (i.e., positions A, B, and C) and the error bars show 1 SD. (a) Net photon response for infrared-stimulated luminescence (IRSL) and blue optically stimulated luminescence (BOSL). (b) IRSL and BOSL depletion ratios. (c) IRSL/BOSL ratio for each depth horizon.

Figures 6 and 7 show the luminescence response of sediment following exposure to gamma rays in cores 2016007PGC018 (sand dominated) and 2016007PGC029 (mud dominated), respectively. Unlike the results from X-radiography, there is evidence for a more systematic increase in net IRSL and BOSL signals following exposure to the gamma-ray source (Figs. 6a and 7a). For horizon-averaged net IRSL signals, the ratios for post–/pre–gamma-ray exposure range from 1.15  $\pm$  0.28 to 2.11  $\pm$  0.30 and 0.82  $\pm$  0.30 to 2.67  $\pm$  2.10 for the sand and mud cores, respectively (Figs. 6a and 7a). For the horizon-averaged net BOSL signals, the post–/pre–gamma-ray exposure ratios range from 0.84  $\pm$  0.25 to 1.24  $\pm$  0.31 and 0.88  $\pm$  0.16 to 2.23  $\pm$  2.17 for the sand and mud cores, respectively (Figs. 6a and 7a).

As with the cores that underwent X-radiography, horizon-averaged IRSL and BOSL depletion ratios remain similar following the exposure of both the sand and mud cores to gamma rays (Figs. 6b and 7b). The same is true for the IRSL/BOSL ratios from the mud core (2016007PGC029), although there is one larger outlier of 1.50  $\pm$  0.50 at the 11 cm horizon (Fig. 7c). By contrast, large

mean increases are seen in two of the three sampled horizons of core 2016007PGC018 (sand) with ratios of  $1.67\pm0.45$  and  $1.88\pm0.29$  (Fig. 6c). Despite this variation in horizon-averaged IRSL/BOSL ratios for post–/pre–gamma-ray exposure for the sand core, the down-core absolute IRSL/BOSL ratios show similar relative changes with depth pre- and post-exposure to the gamma-ray logger (Supplementary Fig. S1). By producing the same relative down-core patterns both pre- and post-exposure, these metrics would provide similar inferences for pOSL profiling despite the wholesale increase in the total magnitude of the luminescence signals caused by gamma irradiation.

# Quartz dosimetry

The quartz dosimeters that underwent X-ray or gamma-ray exposure received doses (Table 2) that were, on average, consistently larger than doses measured from 0 Gy calibration quartz, which has a mean dose of  $6.41 \pm 0.06$  mGy (Table 2). That the "0 Gy" calibration quartz yielded a measurable dose may be an artefact of the rapid method used here to estimate radiation exposure or

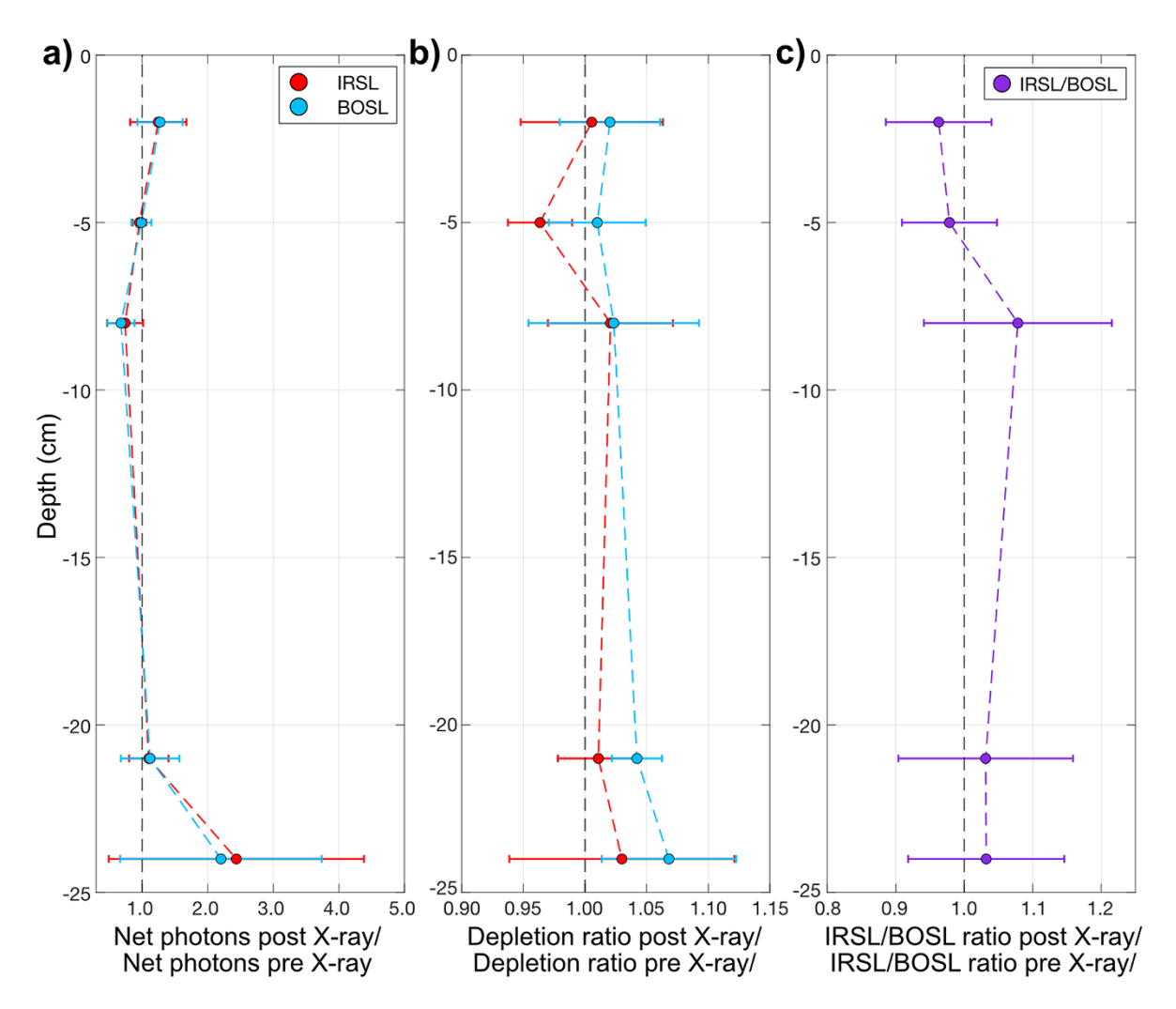


Figure 5. Luminescence data vs. depth, from box core 2016007PGC26 (mud dominated, exposed to X-rays). Symbols and uncertainty are the same as Figure 4. (a) Net photon response for infrared-stimulated luminescence (IRSL) and blue optically stimulated luminescence (BOSL). (b) IRSL and BOSL depletion ratios. (c) IRSL/BOSL ratio for each depth horizon.

may be due to the calibration quartz having been in storage for several years since being zeroed. The X-radiograph also delivers smaller doses than the gamma-ray logger, on average. For the X-radiograph, average doses are  $16.26 \pm 2.66$  mGy in sand and  $25.96 \pm 5.88$  mGy in mud, compared with  $80.36 \pm 10.52$  mGy in sand and  $39.11 \pm 18.75$  mGy in mud following gamma-ray exposure.

For all cores except core 2016007PGC017, position C received the highest average doses (Table 2). However, similar to the net pOSL signals, there is considerable variability in results across different sample positions. For instance, doses for core 2016007PGC018 range across an order of magnitude from  $14.84 \pm 7.89$  mGy in position A to  $156.79 \pm 29.82$  mGy in position C.

## The effect of water content on pOSL profiling signals

Increasing water content leads to a significant decrease in net IRSL and BOSL signals by as much as  ${\sim}60\%$  in the finer sediment and  ${\sim}70\%$  in the coarser sediment at 30% water content (Fig. 8a). Even a 10% increase in water content results in a 20–30% difference in net photon signals for sand- and mud-sized sediment. We observe a gradual increase in net photon signals beyond 30–50%

water content by as much as 20% in the case of the mud-sized sediment. The depletion ratios and IRSL/BOSL ratios are less sensitive to water content than net IRSL and BOSL signals. Generally, there is a slight decrease in both IRSL and BOSL depletion ratios with increasing moisture content (Fig. 8b). However, this decrease remains <10% for all water content tested except for two outliers. Specifically, in the IRSL signal of mud at 5% water that resulted in a signal increase of  $\sim\!60\%$  and the IRSL signal of sand at 10% water that resulted in a signal decrease of  $\sim\!30\%$  (Fig. 8b). The IRSL/BOSL ratio is scattered around unity with no clear trend in either the sand- or mud-sized sediment with increasing water content (Fig. 8c). Although, like the depletion ratios, this scatter remains mostly within <10% of the dry sample.

# **Discussion**

#### The impact of ionising radiation sources on pOSL metrics

Our results show that gamma-ray logging causes a greater change in pOSL signals than X-radiography. This is demonstrated both by (1) an overall greater increase in net IRSL and BOSL signals relative to pre-dosing signals for gamma exposure (Fig. 3), and (2) greater

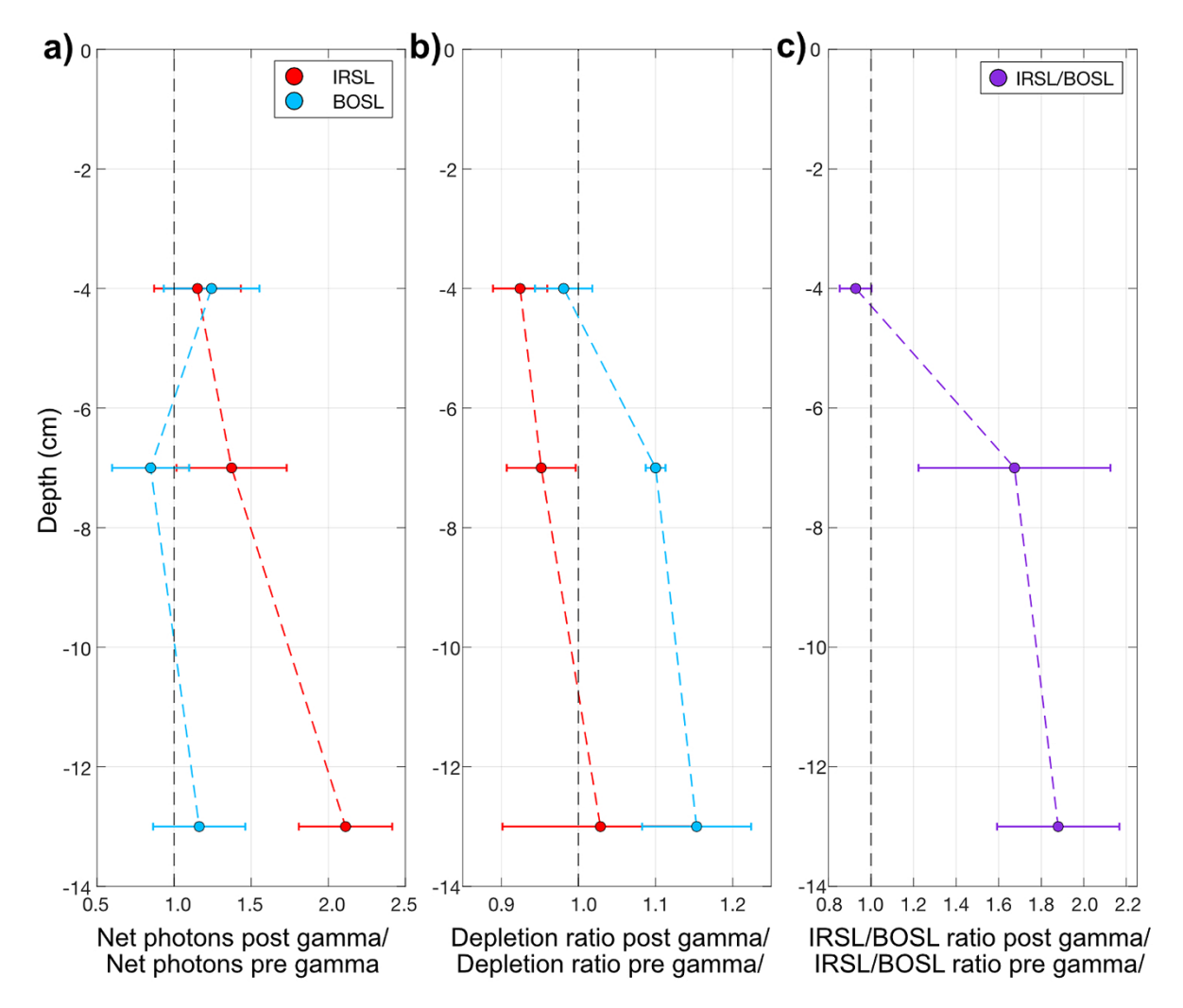


Figure 6. Luminescence data vs. depth from box core 2016007PGC18 (sand dominated, exposed to gamma rays). Symbols and uncertainty are the same as Figure 3. (a) Net photon response for infrared-stimulated luminescence (IRSL) and blue optically stimulated luminescence (BOSL). (b) IRSL and BOSL depletion ratios. (c) IRSL/BOSL ratio for each depth horizon.

gamma doses estimated using calibration quartz (Table 2). These findings are unsurprising given the greater energy of gamma rays compared with X-rays, and the longer exposure time and closer proximity of the source as the core passes through the gamma-ray logger.

Despite the greater impact of gamma-ray logging on net pOSL signals, most post-irradiation measurements overlap with or lie within ±10% of unity of pre-dosed pOSL signals when uncertainties are considered (Figs. 6a and 7a). Therefore, changes in luminescence signals due to dosing exposure are limited in magnitude. Given the steps taken to minimise inter-aliquot variability arising from instrumental setup, such as making sure aliquots were level and positioned in the centre of the pOSL reader sample chamber, the observed scatter in net photon counts likely relates to natural variability in pOSL signals across core horizons (Fig. 3). This interaliquot signal variability possibly results from two principal factors. First, there is often considerable variability in the luminescence signals of water-lain sediments resulting from poor resetting during transport (Berger, 1990; Rittenour, 2008). This is expected to be especially prevalent in marine settings, like the Bute Inlet, due to the depth of the water column limiting light penetration (Armitage, 2015). Second, variability is enhanced by the small surface area (1

cm<sup>2</sup>) of each sample. Larger sample sizes incorporate the signal of more grains, meaning that smaller sample sizes often reveal more inter-sample heterogeneity (Duller, 2008a). Luminescence profiling studies typically use sediment samples spread over the surface of a 5-cm-diameter petri dish fit to pOSL sample drawers. Studies with a 5 cm sample area show good repeatability between absolute signal counts for sediments from the same horizons (e.g., Nitundil et al., 2023). Both of these factors mean that the small doses  $(10^0-10^2 \text{ mGy}; \text{Table 2})$  delivered by the radiation sources used here are likely not large enough to overprint the natural variability of sampling water-lain sediment.

While this study is, to the best of our knowledge, the first time that the influence of a gamma-ray logger on luminescence signals has been tested, our X-radiography dosimetry results agree well with previous findings. Average doses of  $16.26 \pm 2.66$  and  $25.96 \pm 5.88$  mGy estimated in the X-ray-exposed cores are similar to those measured by Davids et al. (2010) at 30 mm depth into a split core following X-radiography (5 mGy). Moreover, doses of 20-40 mGy were measured by dosimeters included in samples during transit to the UK from Cambodia by Sanderson et al. (2007). Of course, the results from different dosimetry studies involving geophysical equipment are not directly comparable because of

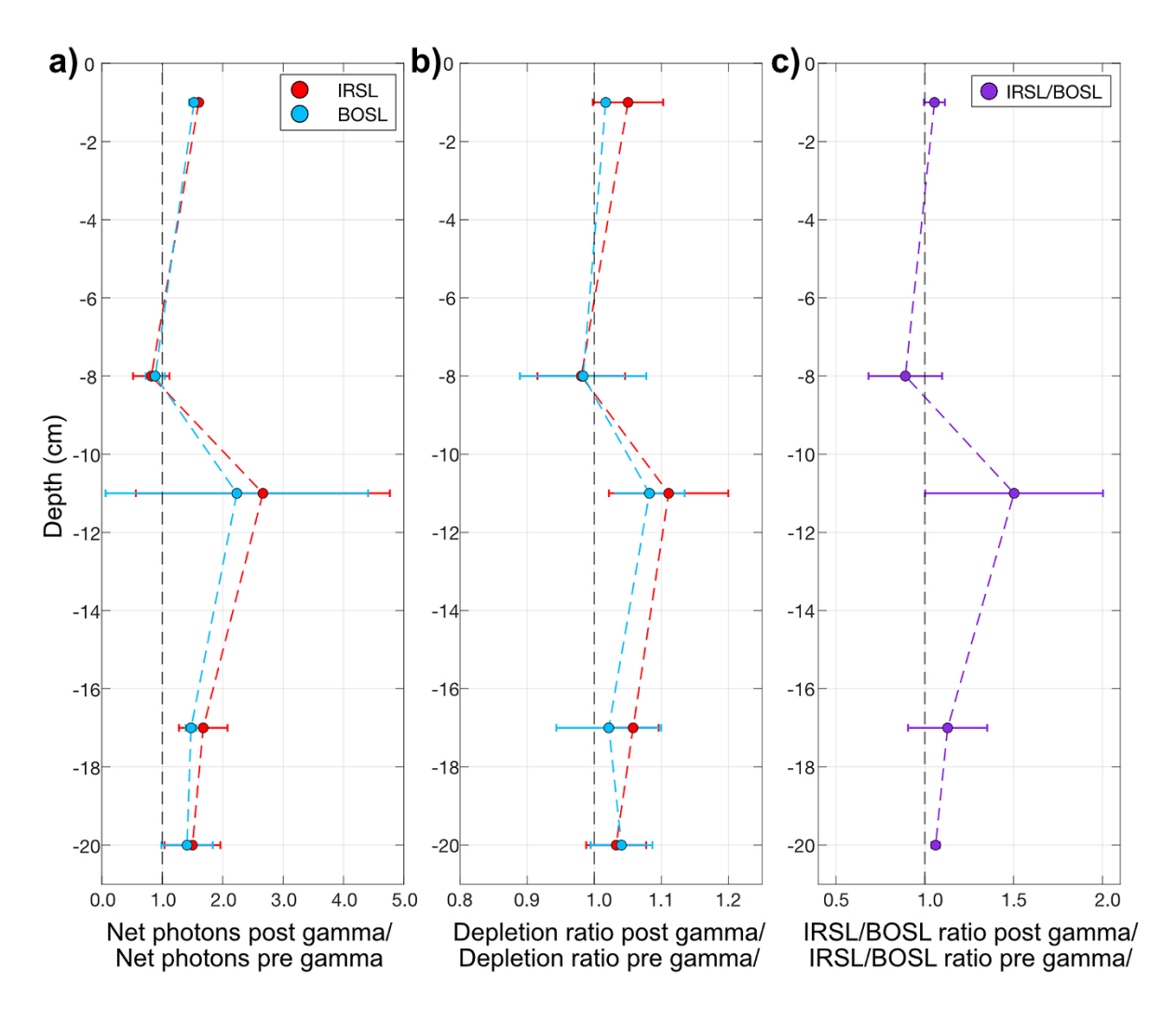


Figure 7. Luminescence data vs. depth from box core 2016007PGC29 (mud dominated, exposed to gamma rays). Symbols and uncertainty are the same as Figure 3. (a) Net photon response for infrared-stimulated luminescence (IRSL) and blue optically stimulated luminescence (BOSL). (b) IRSL and BOSL depletion ratios. (c) IRSL/BOSL ratio for each depth horizon.

different experimental setups (e.g., different radiation sources, distances, and exposure times). However, good relative agreement shows that sealed core sediments are minimally impacted by X-radiograph exposure beyond the depth of several millimetres. Our results are several orders of magnitude lower than those measured at the surfaces of split cores exposed to X-radiography (up to 609 mGy; Davids et al., 2010) and materials exposed to portable and benchtop XRF, which yielded changes in net pOSL signals up to 46 times greater than pre-exposure signals (Huntley et al., 2016). While larger individual sample doses are typically estimated following gamma-ray exposure (up to  $156.79 \pm 29.82$  mGy; Table 2), horizon-averaged doses are of a similar order of magnitude as those from X-radiography ( $39.11 \pm 18.75$  and  $80.36 \pm 10.52$  mGy; Table 2).

Unlike Davids et al. (2010), we do not observe that samples in the centre of cores (position B in our study; Fig. 2) yield the largest increases in pOSL signals (Fig. 3) or receive greater doses of radiation, relative to samples on either side (positions A and C in our study; Fig. 2; Table 2). This difference is perhaps because we tested the impact of exposure on sealed cores, rather than a split core with a flat surface. The more complex geometry of a sealed core means that the outer positions (A and C) are less shielded

than position B samples, given the shallower depth of sediment and water at the edges of the cylindrical shape. So, despite being less proximal to the beam emitted by the radiation source that is more concentrated at its centre than at the edges, outer edges may receive higher doses. This discrepancy may also be due to the centre line of the core (and the quartz dosimeters sealed inside) being imperfectly aligned perpendicular to the sources, despite our best efforts. It is unlikely that archived cores, which have already undergone geophysical logging, would have detailed information about their alignment relative to radiation sources, beyond assuming they were subject to standard practice at the storage facility. So, if the variability among our results is due to imperfect alignment, then it likely simulates the processing methodology for most archived

Taken together, our pOSL signal and dosimetry results show that the exposure of sediment cores to X-radiography and gammaray logging makes very little difference to their luminescence signals. This can be contextualised in terms of the age overestimation that would result if exposed samples underwent subsequent luminescence dating. Using the doses measured by the calibration quartz dosimeters and an environmental dose rate of 2.00 Gy/ka (within the typical range for most sediments; Mahan et al.,

**Table 2.** Estimated doses from calibration quartz sealed inside cores before exposure to X-radiography or gamma-ray logging, as well as blank controls.<sup>a</sup> Results are shown for positions A, B and C within cores and uncertainties are given as standard errors. For the purpose of contextualising the theoretical impact of these doses on luminescence ages, a hypothetical environmental dose rate of 2.00 Gy/ka was used to calculate an equivalent mean age in years.

	Source	Estimated dose by sample position (mGy)				
Core		A	В	С	Mean estimated dose (mGy)	Equivalent mean age <sup>b</sup> (years)
2016007PGC017	X-radiograph	22.30 ± 11.03	15.36 ± 2.93	11.11 ± 1.69	16.26 ± 2.66	8.13 ± 1.33
2016007PGC026	X-radiograph	30.80 ± 17.61	11.79 ± 3.28	35.28 ± 24.24	25.96 ± 5.88	12.98 ± 2.94
2016007PGC018	Gamma-ray logger	14.84 ± 7.89	69.47 ± 7.17	156.79 ± 29.82	80.36 ± 10.52	40.18 ± 5.16
2016007PGC029	Gamma-ray logger	24.92 ± 12.84	8.37 ± 0.58	84.04 ± 15.66	39.11 ± 18.75	19.56 ± 9.38
Blank quartz	NA	NA	NA	NA	6.41 ± 0.06	3.20 ± 0.03

<sup>&</sup>lt;sup>a</sup>Results are shown for positions A, B, and C within cores, and uncertainties are given as standard errors

<sup>&</sup>lt;sup>b</sup>For the purpose of contextualising the theoretical impact of these doses on luminescence ages, a hypothetical environmental dose rate of 2.00 Gy/ka was used to calculate an equivalent mean age in years.

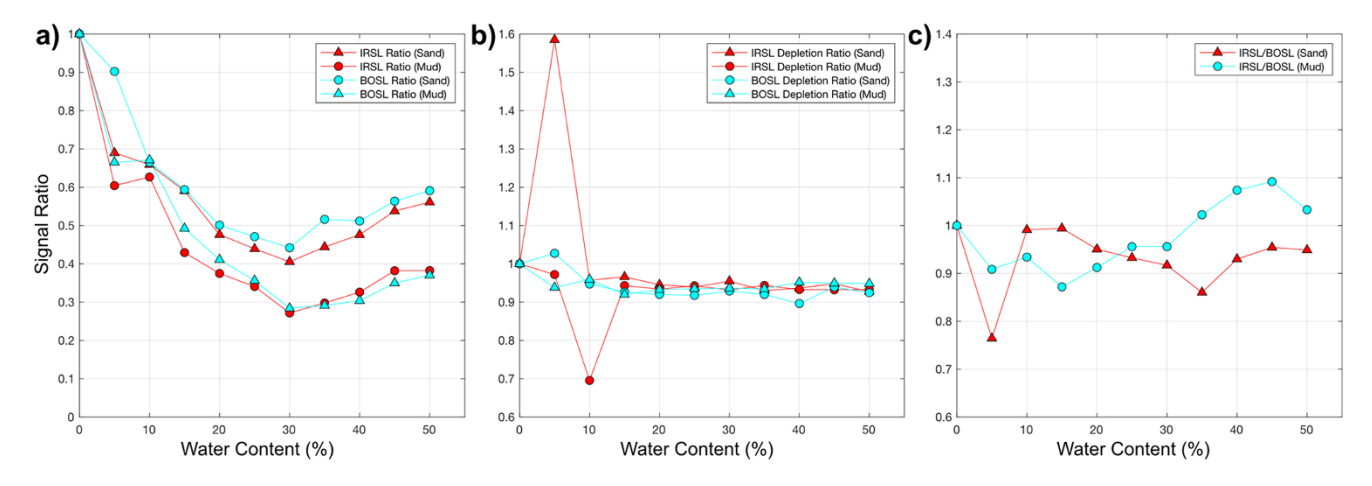


Figure 8. The response of luminescence characteristics to increasing water content by % mass for sand- and mud-sized sediment. (a) Net infrared-stimulated luminescence (IRSL) and blue optically stimulated luminescence (BOSL)counts, (b) IRSL and BOSL depletion ratios, and (c) IRSL/BOSL ratios. In all panels, the portable optically stimulated luminescence (pOSL) signal is expressed as a ratio with the dry sample (so at 0% water content, the ratio is equal to 1).

2023) gives average ages of  $\sim$ 8–13 years and  $\sim$ 20–40 years following X-radiography and gamma-ray logging, respectively (Table 2). With respect to the usual timescales in question for luminescence dating ( $10^3$ – $10^5$  years; Durcan and Woor, 2025), such additional doses would be inconsequential to the accuracy of ages and smaller than age uncertainties arising from other factors (typically 5–10%; Duller, 2008b). It is important to acknowledge that environmental dose rates vary between contexts, but even a low dose rate of 0.5 Gy/ka (Mahan et al., 2023) would only result in the addition of  $\sim$ 32–52 years and  $\sim$ 80–200 years for the X-radiography and gamma-ray logger, respectively.

The effect of geophysical logging not only causes negligible impact to the potential dating of core sediments, but also to subsequent luminescence signal profiling. The depletion ratios and IRSL/BOSL ratios showed very little change following exposure to the radiation sources (Figs. 4–7). The absolute magnitudes of both depletion ratios and IRSL/BOSL ratios, relative to each other down-core, also show consistent down-core patterns preand post-dosing (Supplementary Fig. S1). Relative changes in relative signal magnitude are typically important in luminescence profiling studies for revealing stratigraphic breaks in sedimentary

characteristics (e.g., Adolph et al., 2022; Roman et al., 2024; Staff et al., 2024). Therefore, the stratigraphic information that can be gleaned from archived core materials that have undergone similar radiation exposures should still be useful for reconstructing sedimentation history. However, caution should be applied if using archived cores that have been subject to ionising radiation to investigate absolute magnitudes of net photon intensities at specific depth horizons. These findings are likely also applicable to sediments that have been subject to other microdosing exposure, such as from X-ray scanners in airports and cosmogenic doses during long-haul flights, with the caveat that these doses will vary due to factors like the different activity of sources and lengths of exposure.

# The impact of variable water content

Variable water content is important to consider when conducting pOSL analyses on sediment cores. While depletion ratios and IRSL/BOSL ratios appear to be broadly insensitive to water content (Fig. 8b and c), our results show that net IRSL and BOSL signals can decrease by as much as  $\sim$ 70% relative to dry sediment at just

30% water content (Fig. 8a). Sediment cores can vary in down-core moisture content (Hennekam and de Lange, 2012), so this variability may obscure changes in net pOSL signals associated with variations in sedimentology. Therefore, while it would slow down luminescence profiling, we suggest that drying sediment samples before pOSL analyses would increase the accuracy of sample comparisons throughout a core. Indeed, small lateral and down-core variations in water content within the marine cores used for the radiation exposure experiments may have also contributed to some of the variability in net signal results (Figs. 1 and 3–7). However, this contribution is likely minimal relative to the effects of variable signal resetting previously discussed, given that water content does not vary so significantly over the small depths and widths of these short cores.

The increase in pOSL signal counts by up to 20% as water content exceeds 30% (Fig. 8a) is likely the result of changes in the surface area of samples due to moisture. Between 0% and 30% water content, the 3 g of sediments became increasingly clumped together when mixed with water, making it difficult to spread in a homogeneous layer across the 5 cm petri dish. After addition of more than 30% water by weight, samples were more readily spread due to their lower viscosity. So the impact of greater moisture content on pOSL signals is not just that water attenuates some of the emitted luminescence, but also that moisture makes it more difficult to standardise samples by surface area. It is important to normalise samples for pOSL analysis by surface area and volume, because more grains exposed to the LEDs means a greater signal emission (Muñoz-Salinas et al., 2011). Drying samples before analysis makes it easier to ensure that a homogenous layer of sediment with a standardised surface area is achievable for each sample, an approach frequently taken in pOSL reader studies (e.g., Bateman et al., 2015, 2018; Robins et al., 2023). Alternatively, a sufficient volume of sediment should be used for each measurement so that the total surface area of each sample is the same, irrespective of viscosity.

#### **Conclusions**

We tested the luminescence response of sand- and mud-sized sediment in archived marine sediment cores following exposure to ionising radiation (X-rays and gamma rays) and as a result of variable water content. We found that exposing sealed cores to Xradiography and gamma-ray logging makes negligible differences to the luminescence signals of sediment collected from the central core. While we did measure increases in net IRSL and BOSL counts following both X-ray and gamma-ray exposure, these increases generally overlap with pre-irradiation measurements within uncertainty and are therefore not statistically significant. We did not observe a greater dose in the central position across core horizons, relative to the outer edges, likely because of the complex shielding geometry of a cylindrical core. On average, the radiation dose received by sediments at the centre of cores was <100 mGy, which is well within the uncertainties of the equivalent doses typical of Holocene and Pleistocene sediments usually dated using luminescence. The trend in relative signal magnitudes down-core, typically used in luminescence profiling studies, was shown to be relatively stable following exposure to radiation sources. Furthermore, depletion ratios and IRSL/BOSL ratios were comparable pre- and post-exposure. We also found that variable water content can be an important limitation to sample comparability, especially when water varies beyond 5% of the total mass of sediment between samples.

These findings show that archived sediment cores have the potential to provide accurate and reliable data for luminescence dating and profiling applications, even if they have previously been subject to ionising radiation exposure or have variable water content. Accurate data likely depend on the following criteria: (1) Sediments are sampled within the central few centimetres of cores where shielding from external radiation sources is greatest, assuming that cores were exposed to ionising radiation before splitting. (2) If inter-sample water content varies by more than a few percent, samples should be dried before analysis. (3) Any previously light-exposed sediments are scraped away from the surfaces of split cores before sampling for luminescence analyses (Armitage and Pinder, 2017).

Our results should be viewed with the caveat that they are based on the radiation sources of geophysical loggers in one laboratory. Different loggers will have different sources, with different strengths, proximities to samples, and exposure times, which will change the doses given to sediments. Moreover, we tested 10-cm-diameter cores of sand- and mud-dominated sediments. Different core diameters, sediment densities and grainsize distributions, and water content will also influence the impact of ionising radiation exposure. The retrospective dosimetry approach employed here, using calibration quartz, provides a repeatable means of estimating doses given by equipment in other laboratories.

**Supplementary material.** The supplementary material for this article can be found at https://doi.org/10.1017/qua.2025.10035.

**Acknowledgments.** This work was supported by funding from the Pacific Rim Ocean Data Mobilization and Technology (PRODIGY) program. MKD gratefully acknowledges funding from the Natural Sciences and Engineering Research Council (NSERC) of Canada (Discovery Grant, no. 2020-05365), the Canada Foundation for Innovation (John R. Evans Leaders Fund Grant, no. 43119), and the British Columbia Knowledge Development Fund. OBL acknowledges support from NSERC Discovery Grant (no. 311281) and NSERC Research Tools and Instruments grants. We thank the guest editor, Shannon Mahan, and two anonymous reviewers for their helpful comments that improved the article.

## References

**Adolph, M.L., Lampe, R., Lorenz, S., Haberzettl, T.**, 2022. Characterization of (paleo) lacustrine landforms using sedimentological and portable OSL investigations at Schweriner See, North-Eastern Germany. *Earth Surface Processes and Landforms* **47**, 422–435.

Algeo, T.J., Phillips, M., Jaminski, J., Fenwick, M., 1994. High-resolution X-radiography of laminated sediment cores. *Journal of Sedimentary Research* 64, 665–668

**Armitage, S.J.**, 2015. Optically stimulated luminescence dating of Ocean Drilling Program core 658B: complications arising from authigenic uranium uptake and lateral sediment movement. *Quaternary Geochronology* **30**, 270, 274

Armitage, S.J., Pinder, R.C., 2017. Testing the applicability of optically stimulated luminescence dating to Ocean Drilling Program cores. *Quaternary Geochronology* 39, 124–130.

Bateman, M.D., Rushby, G., Stein, S., Ashurst, R.A., Stevenson, D., Jones, J.M., Gehrels, W.R., 2018. Can sand dunes be used to study historic storm events?. *Earth Surface Processes and Landforms* **43**, 779–790.

Bateman, M.D., Stein, S., Ashurst, R.A., Selby, K., 2015. Instant luminescence chronologies? High resolution luminescence profiles using a portable luminescence reader. *Quaternary Geochronology* **30**, 141–146.

Berger, G.W., 1990. Effectiveness of natural zeroing of the thermoluminescence in sediments. *Journal of Geophysical Research*: *Solid Earth* **95**(B8), 12375–12397.

Berger, G.W., 2009. Zeroing tests of luminescence sediment dating in the Arctic Ocean: review and new results from Alaska-margin core tops and central-ocean dirty sea ice. *Global and Planetary Change* **68**(1–2), 48–57.

- Burrough, S.L., Thomas, D.S., Bailey, R.M., 2009. Mega-Lake in the Kalahari: a Late Pleistocene record of the Palaeolake Makgadikgadi system. *Quaternary Science Reviews* 28, 1392–1411.
- Davids, F., Roberts, H.M., Duller, G.A., 2010. Is X-ray core scanning non-destructive? Assessing the implications for optically stimulated luminescence (OSL) dating of sediments. *Journal of Quaternary Science* 25, 348–353
- Duller, G.A., 2008b. Luminescence Dating: Guidelines On Using Luminescence Dating In Archaeology. English Heritage Trust, Swindon, UK.
- **Duller, G.A.**, 2008a. Single-grain optical dating of Quaternary sediments: why aliquot size matters in luminescence dating. *Boreas* **37**, 589–612.
- Durcan, J.A., Woor, S., 2025. Quartz optical dating. In: Elias, S. (Ed.), Encyclopaedia of Quaternary Science. 3rd ed. Vol. 1. Elsevier, London, pp. 751–764.
- Gray, H.J., Jain, M., Sawakuchi, A.O., Mahan, S.A., Tucker, G.E., 2019.
  Luminescence as a sediment tracer and provenance tool. Reviews of Geophysics 57, 987–1017.
- Hage, S., Galy, V.V., Cartigny, M.J., Heerema, C., Heijnen, M.S., Acikalin, S., Clare, M.A., et al., 2022. Turbidity currents can dictate organic carbon fluxes across river-fed fjords: an example from Bute Inlet (BC, Canada). Journal of Geophysical Research: Biogeosciences 127, e2022JG006824.
- Hansen, V., Murray, A., Buylaert, J.P., Yeo, E.Y., Thomsen, K., 2015. A new irradiated quartz for beta source calibration. *Radiation Measurements* 81, 123–127.
- Hansen, V., Murray, A., Thomsen, K., Jain, M., Autzen, M., Buylaert, J.P., 2018. Towards the origins of over-dispersion in beta source calibration. *Radiation Measurements* 120, 157–162.
- Hennekam, R., de Lange, G., 2012. X-ray fluorescence core scanning of wet marine sediments: methods to improve quality and reproducibility of high-resolution paleoenvironmental records. *Limnology and Oceanography: Methods* 10, 991–1003.
- Huntley, D.J., Godfrey-Smith, D.I., Thewalt, M.L., 1985. Optical dating of sediments. Nature 313, 105–107.
- Huntley, J., Westaway, K.E., Gore, D.B., Aubert, M., Ross, J., Morwood, M.J., 2016. Non-destructive or noninvasive? The potential effect of X-ray fluorescence spectrometers on luminescence age estimates of archaeological samples. *Geoarchaeology* 31, 592–602.
- Kluesner, J.W., Johnson, S.Y., Nishenko, S.P., Medri, E., Simms, A.R., Greene, H.G., Gray, H.J., et al., 2023. High-resolution geophysical and geochronological analysis of a relict shoreface deposit offshore central California: implications for slip rate along the Hosgri fault. Geosphere 19, 1–24.
- Kreutzer, S., Schmidt, C., Fuchs, M.C., Dietze, M., Fischer, M., Fuchs, M., 2012. Introducing an R package for luminescence dating analysis. *Ancient TL* 30, 1–8.
- Mahan, S.A., Rittenour, T.M., Nelson, M.S., Ataee, N., Brown, N., DeWitt, R., Durcan, J., et al., 2023. Guide for interpreting and reporting luminescence dating results. GSA Bulletin 135, 1480–1502.
- Muñoz-Salinas, E., Bishop, P., Sanderson, D.C., Zamorano, J.J., 2011. Interpreting luminescence data from a portable OSL reader: three case studies in fluvial settings. *Earth Surface Processes and Landforms* **36**, 651–660.
- Munyikwa, K., Kinnaird, T.C., Sanderson, D.C., 2021. The potential of portable luminescence readers in geomorphological investigations: a review. *Earth Surface Processes and Landforms* **46**, 131–150.
- Murray, A., Arnold, L.J., Buylaert, J.P., Guérin, G., Qin, J., Singhvi, A.K., Smedley, R., Thomsen, K.J., 2021. Optically stimulated luminescence dating using quartz. *Nature Reviews Methods Primers* 1, 72.
- Murray, A.S., Thomsen, K.J., Masuda, N., Buylaert, J.P., Jain, M., 2012. Identifying well-bleached quartz using the different bleaching rates of quartz and feldspar luminescence signals. *Radiation Measurements* 47, 688–695.
- Nitundil, S., Stone, A., Srivastava, A., 2023. Applicability of using portable luminescence reader for rapid age-assessments of dune accumulation in the Thar desert, India. *Quaternary Geochronology* 78, 101468.

Pears, B., Brown, A.G., Toms, P.S., Wood, J., Sanderson, D., Jones, R., 2020. A sub-centennial-scale optically stimulated luminescence chronostratigraphy and late Holocene flood history from a temperate river confluence. *Geology* 48, 819–825.

- Rex, C.L., Staff, R.A., Sanderson, D.C., Cresswell, A.J., Marshall, M.H., Hyodo, M., Horiuchi, D., Tada, R., Nakagawa, T., 2022. Controls on luminescence signals in lake sediment cores: a study from Lake Suigetsu, Japan. *Quaternary Geochronology* 71, 101319.
- Rittenour, T.M., 2008. Luminescence dating of fluvial deposits: applications to geomorphic, palaeoseismic and archaeological research. *Boreas* 37, 613–635.
- Robins, L., Greenbaum, N., Yu, L., Bookman, R., Roskin, J., 2021. High-resolution portable-OSL analysis of Vegetated Linear Dune construction in the margins of the northwestern Negev dunefield (Israel) during the late Quaternary. *Aeolian Research* 50, 100680.
- Robins, L., Roskin, J., Marder, O., Edeltin, L., Yu, L., Greenbaum, N., 2023. Geomorphic, environmental, and archeological significance of Last Glacial Maximum to middle Holocene dune damming, northwestern Negev dunefield margin, Israel. *Quaternary Science Reviews* 308, 108098.
- Roman, M., Píšková, A., Sanderson, D.C., Cresswell, A.J., Bulínová, M., Pokorný, M., Kavan, J., et al., 2024. The Late Holocene deglaciation of James Ross Island, Antarctic Peninsula: OSL and 14C-dated multi-proxy sedimentary record from Monolith Lake. Quaternary Science Reviews 333, 108693
- Rothwell, R.G., Rack, F.R., 2006. New techniques in sediment core analysis: an introduction. *Geological Society of London Special Publication* **267**, 1–29.
- Sanderson, D.C., Murphy, S., 2010. Using simple portable OSL measurements and laboratory characterisation to help understand complex and heterogeneous sediment sequences for luminescence dating. *Quaternary Geochronology* 5, 299–305.
- Sanderson, D.C., Bishop, P., Stark, M., Alexander, S., Penny, D., 2007.Luminescence dating of canal sediments from Angkor Borei, Mekong Delta, southern Cambodia. *Quaternary Geochronology* 2, 322–329.
- Schmidt, C., Sanderson, D.C.W., Cresswell, A., Chruścińska, A., Fasoli, M., Polymeris, G., Kreutzer, S., Biernacka, M., Adamiec, G., Martini, M., 2021. A systematic multi-technique comparison of two reference quartz samples. Special Issue: LED2021 Abstracts, Ancient TL 39(S).
- Sohbati, R., Murray, A., Lindvold, L., Buylaert, J.P., Jain, M., 2017.
  Optimization of laboratory illumination in optical dating. *Quaternary Geochronology* 39, 105–111.
- Staff, R.A., Sanderson, D.C., Rex, C.L., Cresswell, A., Hyodo, M., Kitaba, I., Marshall, M.H., et al., 2024. A luminescence-derived cryptostratigraphy from the Lake Suigetsu sedimentary profile, Japan: 45,000–30,200 IntCal20 yr BP. Quaternary Geochronology 83, 101588.
- Stokes, S., Bray, H.E., 2005. Late Pleistocene eolian history of the Liwa region, Arabian Peninsula. Geological Society of America Bulletin 117, 1466–1480.
- Stokes, S., Ingram, S., Aitken, M.J., Sirocko, F., Anderson, R., Leuschner, D., 2003. Alternative chronologies for Late Quaternary (Last Interglacial–Holocene) deep sea sediments via optical dating of silt-sized quartz. Quaternary Science Reviews 22, 925–941.
- Stone, A., Bateman, M.D., Burrough, S.L., Garzanti, E., Limonta, M., Radeff, G., Telfer, M.W., 2019. Using a portable luminescence reader for rapid age assessment of aeolian sediments for reconstructing dunefield landscape evolution in southern Africa. *Quaternary Geochronology* 49, 57–64.
- Stone, A., Bateman, M.D., Sanderson, D., Burrough, S.L., Cutts, R., Cresswell, A., 2024. Probing sediment burial age, provenance and geomorphic processes in dryland dunes and lake shorelines using portable luminescence data. *Quaternary Geochronology* 82, 101542.
- Tjallingii, R., Röhl, U., Kölling, M., Bickert, T., 2007. Influence of the water content on X-ray fluorescence core-scanning measurements in soft marine sediments. *Geochemistry, Geophysics, Geosystems* 8. https://doi.org/10.1029/ 2006GC001393.
- Weltje, G.J., Tjallingii, R., 2008. Calibration of XRF core scanners for quantitative geochemical logging of sediment cores: theory and application. *Earth and Planetary Science Letters* 274, 423–438.
- Wintle, A.G., Huntley, D.J., 1979. Thermoluminescence dating of a deep-sea sediment core. *Nature* 279, 710–712.